



# SYNTHESIS, CHARACTERIZATION, PHOTOLUMINESCENCE STUDIES OF 8-HYDROXYQUINOLINE COPOLYMERS AND ITS CARBON COMPOSITES

Yashpal U. Rathod<sup>1</sup>, Anup K. Parmar<sup>1</sup>, Rahul R. Kurzekae<sup>1</sup>, Wasudeo B. Gurnule<sup>2\*</sup>

<sup>1</sup>Department of Chemistry, C. J. Patel College Tirora - 441911, India

<sup>2\*</sup>Department of Chemistry, Kamla Nehru Mahavidyalaya, Nagpur-440024, India

\*Wasudeo Gurnule: Email: [wbgurnule@gmail.com](mailto:wbgurnule@gmail.com)

## Abstract:

8-hydroxyquinoline5-sulphonic acid, anthranilic acid and formaldehyde were utilized to create the copolymer and activated charcoal were utilized to synthesized the new composite. The properties and structure of the copolymer and the copolymer/activated charcoal composite were assessed using a variety of characterisation methods such as UV-Visible, FTIR, NMR (<sup>1</sup>H & <sup>13</sup>C) spectra, elemental analysis, and SEM. Gel permeation chromatography were utilized for determination of molecular weight distribution. Photoluminescence was used to study their fluorescence characteristics, and the results showed that the photoluminescence wavelength of the composite changed to red in comparison to that of the copolymer.

**Keywords:** copolymer; composite; photoluminescence studies; polycondensation; elemental analysis.

## 1. Introduction:

The last several years have seen an increase in attention in polymer-based rare earth luminescent materials[1], as these materials offer the benefits of both rare earth compound luminescence properties, characteristics include lengthy luminescence durations, distinct emission bands, significant Stokes shifts, and elevated quantum yields, as well as the physical attributes of polymers, like their strength, flexibility, and processability. Most of the ground-breaking research in this area has

focused on polymer systems that have been mixed or doped with lanthanide chemicals [2].

A significant contribution to the advancement of science and technology may come from luminescent materials with quantum efficiencies greater than unity. Numerous scientific disciplines, including biotechnology, diagnostics, cell biology, pharmaceuticals, and analytics are very interested in nanoparticles [3]. Due to the improved thermal and mechanical properties of the composites, the production and development of nanocomposites based on polymers has recently acquired prominence. Additionally, the composition of the matrix has an impact on the functional characteristics of the nanocomposites. In numerous medicinal, agricultural, drug release, and packaging applications [4, 5], polymer-based nanocomposites exhibit outstanding benefits of biodegradability and biocompatibility.

The hydroxyl-group containing polymers are among the most desirable for encasing ZnS semiconductor nanocrystals [6-7]. Wang et al. recently reported multi-layered ZnS:Cu nanoparticles made of chitosan and alginate as well as ZnxCd1-xS/alginate nanoparticles with an alginate coating [8-9]. Gurnule et al. investigated the photoluminescence characteristics of a novel copolymer composite, which was created by ultrasonically mixing activated charcoal in a 1:2 molar ratios with 2-amino 6-nitrobenzothiazole/melamine/8-hydroxyquinoline5-sulphonic acid/ phthalic acid/formaldehyde copolymer. The copolymer

produces strong blue light with a wavelength of 440 nm when activated at 365 nm, which is suitable for OLEDs [10-11]. Desai and colleagues [12] used oxidative coupling polymerization to create a new functional alternating copolymer with well-defined pyrrole and anthracene units in the main chain. The copolymer fluorescence spectra in solid powder were found to have anthracene concentrations and were highest at 518 nm, in the green region. By using a direct chemical oxidative polymerization process, copolymers of polypyrrole with various moieties such as pyrene, fluorene, thiophene, carbazole, and terephthalaldehyde were created [13–16]. When compared to their homomers, the produced copolymers showed unique thermal, electrical, and fluorescence characteristics [13-15].

## 2. Experimental

### 2.1 SYNTHESIS OF COPOLYMER AND COMPOSITE

Following a process based on prior literature [16], the 8-hydroxyquinoline-5-sulphonic acid (0.2 mol), anthranilic acid (0.1 mol), and formaldehyde (0.5 mol) copolymer was created utilising the polycondensation method on acid medium for 6 h at 124 °C in an oil bath. Fig.1 depicts the copolymer synthesis mechanism. A composite made of a new copolymer and activated charcoal was created in a 1:2 ratio. The activated charcoal was added after the copolymer had been dissolved in 25 ml of DMF, and the mixture was then ultrasonically processed for 3 hours with continuous stirring for 24 hours. Lastly the dark colored composite was dried in an air oven at 70°C for 24 hrs

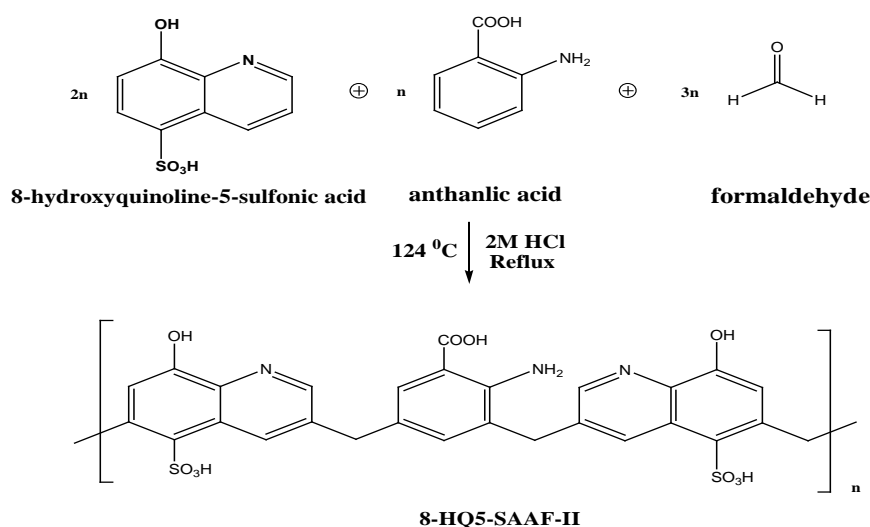


Figure 1: structure of 8-HQ5-SAAF-II copolymer.

## 3. Results and Discussion

### 3.1 Elemental analysis

The 8-HQ5-SAAF-II copolymers were investigated for C, H, N, and S. The assessed values and the noticed discoveries are viewed as Table 1: Elemental analysis data of copolymer

Compound	Elemental Analysis (%)				Empirical Formulae of Repeating Unit	Formulae Mass
	Found (Calculated)					
	C	H	N	S		
8-HQ5-SAAF-II	54.00 (53.00)	3.08 (3.43)	6.76 (6.8)	10.38 (10.74)	C <sub>29</sub> H <sub>25</sub> N <sub>3</sub> O <sub>10</sub> S <sub>2</sub>	611

### 3.2 Molecular weight determination

It is determined that there is a good degree of agreement between the evaluated and observed values. The empirical formula was

in great agreement [17]. The empirical weight of a single repeating unit was computed using the empirical formula. Table 1 provides analytical information for all four 8-HQ5-SAAF-II copolymers.

used to calculate the empirical weight of a single repeating unit. Table 2 provides analytical information for 8-HQ5-SAAF-II copolymers. GPC (Shimadzu, Japan) assessed

the molecular weights of the copolymer's number average ( $\bar{M}_n$ ) weight average ( $\bar{M}_w$ ) and size average ( $\bar{M}_z$ ) using THF as a mobile phase

Table 2: Molecular weight data of copolymer

Copolymer	Weight average molecular weight $\bar{M}_w$	Number average molecular weight $\bar{M}_n$	Size average molecular weight $\bar{M}_z$	The polydispersity index $\frac{\bar{M}_w}{\bar{M}_n}$	The polydispersity index $\frac{\bar{M}_z}{\bar{M}_w}$
(8-HQ5-SAAF)-II	6869	6884	6899	1.0027	1.0029

### 3.3 UV-Visible spectra

The copolymer spectrum revealed two unique absorption bands at 470 nm and 280 nm, which are attributed to the  $n \rightarrow \pi^*$  and  $\pi \rightarrow \pi^*$  transitions, respectively. The intensity of these absorption bands varied, with the band at 280 nm showing the lowest intensity. This band is less strong and is centered at 280 nm. It is caused by the ( $\pi \rightarrow \pi^*$ ) allowed transition of chromophore groups that are in conjugation with an aromatic nucleus [18]. On the other hand, the  $n \rightarrow \pi^*$  transition of -NH groups is responsible for the strong band observed at 470 nm. The presence of the aromatic nucleus is confirmed by the  $\pi \rightarrow \pi^*$  transition, while the

presence of the -NH groups is demonstrated by the  $n \rightarrow \pi^*$  transition.

As illustrated in Fig. 2, the copolymer composite's spectrum revealed two absorption bands at 260 nm and 470 nm. The presence of a carbonyl group and an aromatic ring in the composite, which may account for the  $\pi \rightarrow \pi^*$  transition, is clearly indicated by the lowered absorbance band at 260 nm and 442 nm. The band at 370 nm assigned to the  $n \rightarrow \pi^*$  transition reveals the presence of the >NH group in the composite [19]. The composite development is confirmed by the observed outcomes due to the shifting of bands. In addition, when compared to the copolymer, the composite absorption has decreased.

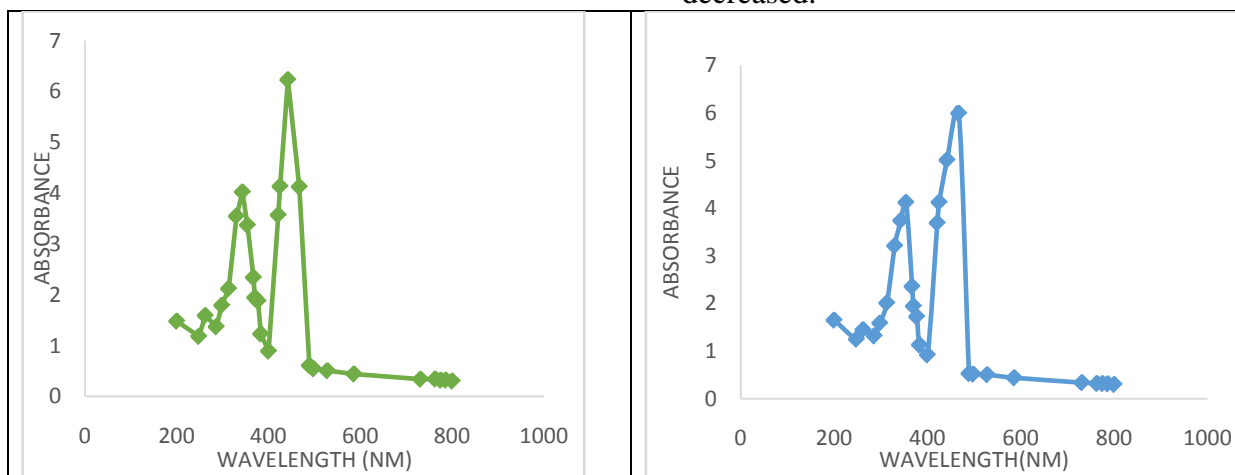


Figure 2: Electronic Spectra of 8-HQ-5-SAAF-II copolymer and its composite

### 3.4 FTIR Spectra

The Fourier transform infrared spectroscopy is the most effective technique for finding the sorts of functional groups and chemical bonds (FTIR). Figure 3 shows the FTIR spectrum of 8-HQ5-SAAF-II copolymer. The hydroxyl group of -COOH present in the aromatic ring is attributed to a broad band in the copolymer spectrum in the range of  $3501 \text{ cm}^{-1}$

[20]. This band appears to have fused with the hydroxyl group of 8-hydroxyquinoline's hydroxyl group. Modes of aromatic ring stretching give rise to a peak at  $3048 \text{ cm}^{-1}$ , while the Ar-NH<sub>2</sub> group's C-N stretching produces a prominent band at  $1271 \text{ cm}^{-1}$ . Between  $1200 \text{ cm}^{-1}$  and  $800 \text{ cm}^{-1}$ , strong, medium-weak, and weak absorption bands of the 1,2,3,5 tetra substitution of the aromatic

benzene ring were visible. Because of the carboxylic ketone's (C=O) stretching vibrations, the band is visible at  $1633\text{ cm}^{-1}$ . Because of the  $\text{CH}_2$  in the copolymer, a weak band can be seen in the area  $3031.1\text{ cm}^{-1}$ . The band that appears to extend an aromatic ring is connected to this band [21].

Figure 3 shows the FTIR spectrum of the 8-HQ5-SAAF-C composite. According to the findings, the composite spectrum differed somewhat from the copolymer spectrum. The broad band at  $3507\text{ cm}^{-1}$  is attributed to the

stretching vibrations of the -OH group induced by the copolymer, whereas the broad band at  $1525.8\text{ cm}^{-1}$  is attributed to the stretching mode of the -NH group caused by the copolymer. This definitely demonstrates composite creation. The - $\text{CH}_2$  linkage was also assigned to the band at  $1310\text{ cm}^{-1}$ , and the stretching vibration of the carbonyl group (C=O) was altered from  $1500\text{ cm}^{-1}$  to  $1650\text{ cm}^{-1}$ . In addition, the aromatic ring stretching mode has shifted from  $3049\text{ cm}^{-1}$  to  $3114\text{ cm}^{-1}$ [22]. At  $1627\text{ cm}^{-1}$ , the C-N stretching vibration appears.

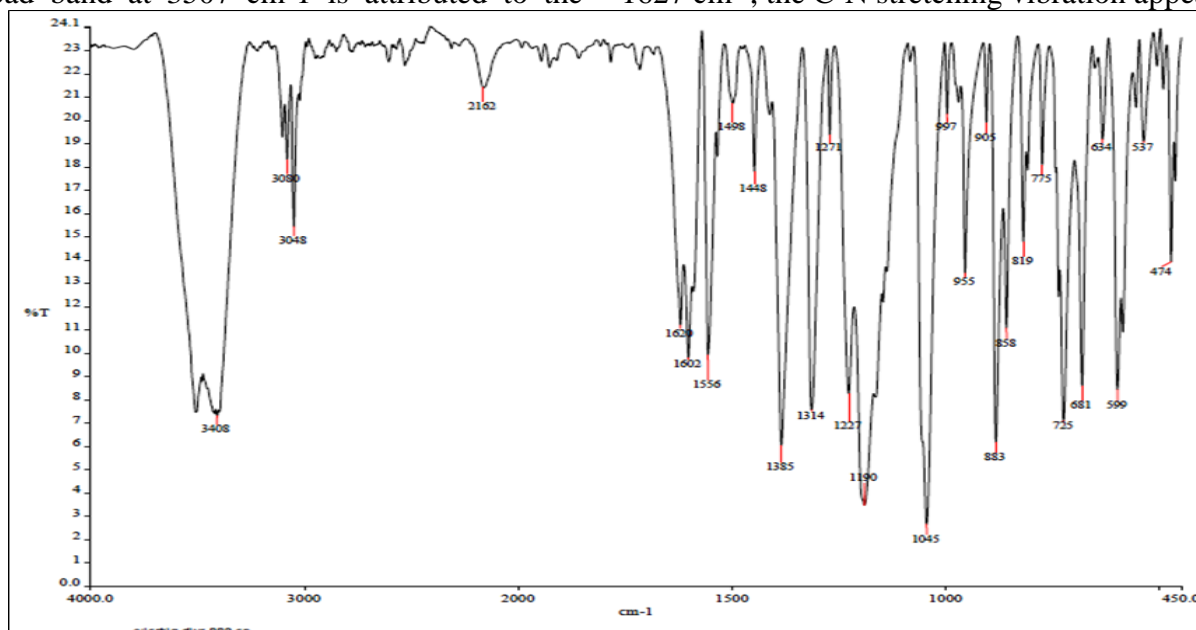


Figure 3: FTIR Spectra of 8-HQ-5-SAAF-II Copolymer

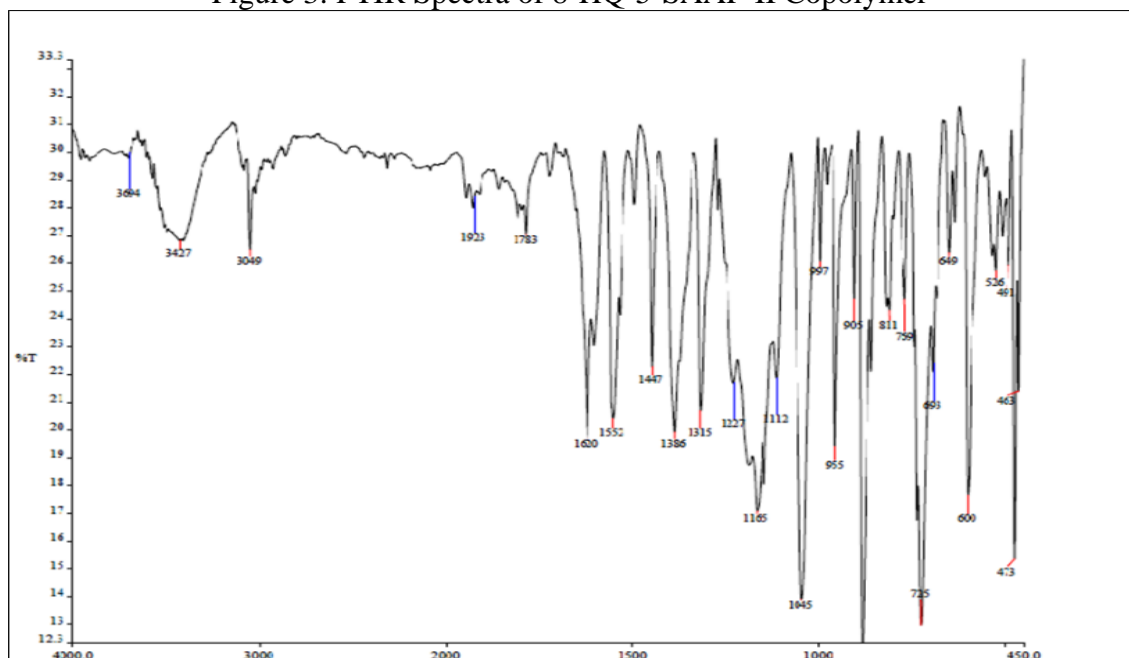


Figure 4: FTIR Spectra of 8-HQ-5-SAAF-II Copolymer Composite

### 3.5 $^1\text{H NMR}$

To support the connections of the suggested structure, the NMR ( $^1\text{H}$ ) spectra of 8-HQ5-SAAF-II copolymers was obtained.

Copolymer 8-HQ5-SAAF proton NMR spectra are shown in (Fig. 4). The Quinoline rings -OH is thought to be responsible for the strong signal at 9.1 ppm. A singlet associated with the -OH of

Ar-COOH that first appeared at 8.6 ppm. The several signals that were found in the range of 7.3 to 8.5 ppm are the anticipated aromatic ring protons [23]. The Ar-CH<sub>2</sub>-Ar bridge's

methylene proton produced a significant signal at 2.4 ppm. The -SO<sub>3</sub>H group is responsible for the sharp singlet that was detected at 9.8 ppm [24].

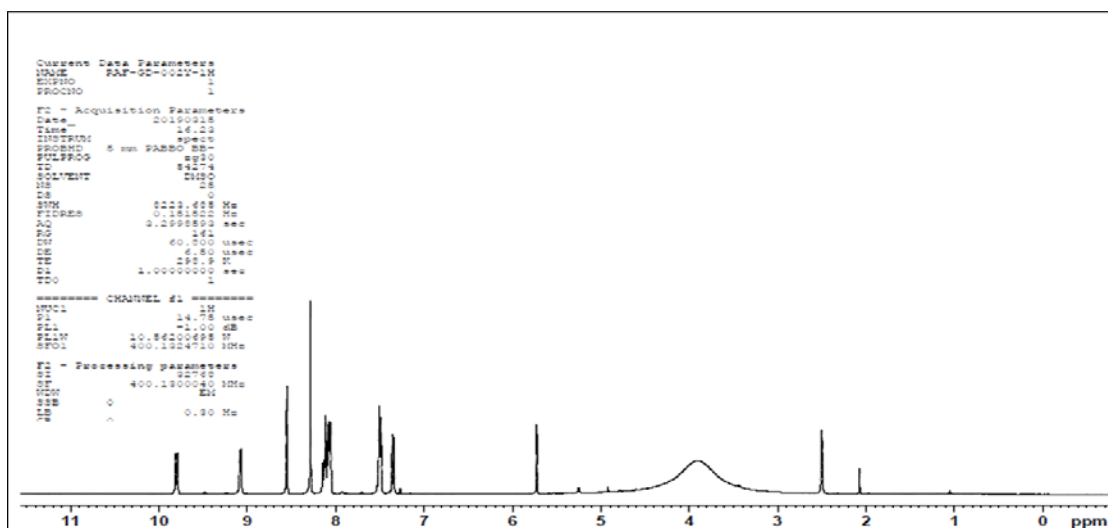


Figure 4: <sup>1</sup>H NMR Spectra of 8-HQ-5-SAAF-II Copolymer

### 3.6 <sup>13</sup>C NMR Spectra

<sup>13</sup>C NMR spectra of the representative copolymer, 8-HQ 5-SAAF, are given in Fig. 5. The literature [25-26] is used to ascribe the observed chemical shifts. The spectrum shows the corresponding peaks at 113.11, 121.98, 125.09, 125.53, 125.70, and 128.3 ppm for the

amino aromatic ring's C1 to C6. The peak at 39.62 ppm was found to be caused by the Ar-CH<sub>2</sub> bridge in the copolymer. In the copolymer, the peaks for C1 to C9 of the quinoline ring were found at concentrations of 148.69, 144.85, 134.89, 130.73, 127.07, 127.91, 127.55, 148.9, and 125.70 ppm, respectively.

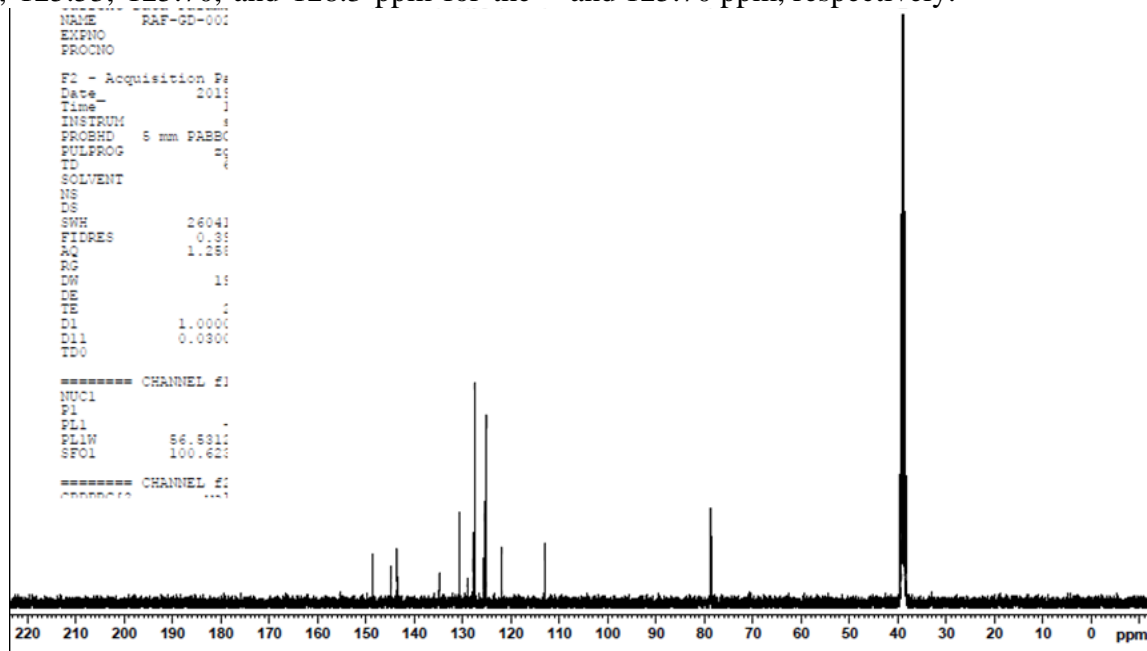


Figure 5: <sup>13</sup>C NMR Spectra of 8-HQ-5-SAAF-II Copolymer

### 3.7 Scanning Electron Microscopy

Samples were examined using a SEM in order to evaluate the morphological properties of the copolymer and its composites. The

obtained pictures are displayed in Fig. 6. The photos reveal tiny nanoparticle clusters adhering to the surface of larger particles. Surface analysis has proven to be quite helpful



in comprehending the material's surface characteristics. A scanning electron microscope was used to examine the morphology of the 8-HQ5-SAAF-II copolymer sample, as shown in Fig. 5.5. There are more active sites and a less densely packed surface on the copolymer surface [27]. The smooth surface resembling white stone was examined in the context of the produced copolymer (fig. 6). There are large gaps in the structure shown in the copolymer micrograph.

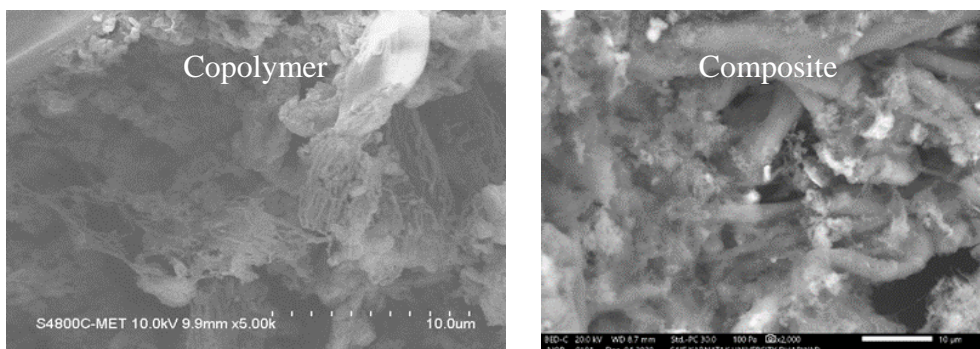


Figure 6: SEM Images of 8-HQ-5-SAAF-II Copolymer and its Composites

### 3.8 Photoluminescence Study

RF-501(PC) S CE (LVD) LS55 Shimadzu MODEL spectrophotometer was used to measure the photoluminescence spectra of copolymer composites at a concentration of 10–4 mol/L in DMF. Fig. 7, 8 displays the photoluminescence spectra of copolymer composites. Copolymer composites shows emission bands in the UV region at 482 nm, along with excitation peak approximately 407 nm (blue), 379 (nm) wavelengths. The PL quenching shows that the rate of photo-induced electron transfer from donor polymer to acceptor charcoal considerably rises with increasing molar ratio of copolymer. Additionally, as the molar ratios of the copolymer in the charcoal rise, a change in the conjugated polymer's effective conjugation causes an increase in the emission of 8-HQ5SAAF-C composites in the blue region [28].

The results of the photoluminescence evaluation for copolymer 8-HQ5-SAAF composites are demonstrated in Fig. PL spectra of this copolymer composite with carbon in this manner demonstrate that the provided material has adequate strength to be used in the study of semiconductor devices. According to the

A little variation in the 8-HQ5-SAAF-CHA composite surface morphology from the copolymer was noted, which could support the composite's development. The composite revealed a less densely packed structure that resembled a sponge with spherulites surface and varying granule sizes. The composite has a larger surface area and a greater variety of cavities available on surface adsorbents. Thus, it can be inferred from this image that the composite including the synthetic polymer and activated charcoal has formed clearly.

findings, the prepared co-appointment copolymer composites can be used as a support material for applications such as strong country lights and picture luminescent fluid display (PLLCD) [29].

The aforementioned discovery makes it evident that the alteration of the copolymer matrix by the addition of charcoal as a filler was the reason why copolymer composites displayed photoluminescence capabilities. With a rise in the molar ratio of the copolymer, the transfer of photo-induced charges from donor copolymer to acceptor charcoal increases effective, suppressing PL emission from the copolymer. As a result, the conducting copolymer-charcoal composites' PL spectra demonstrate that the material was of sufficient quality to be used in semiconductor device research and serve as a support material for applications such as solid-state lighting and photoluminescent liquid crystal displays (PLLCDs).

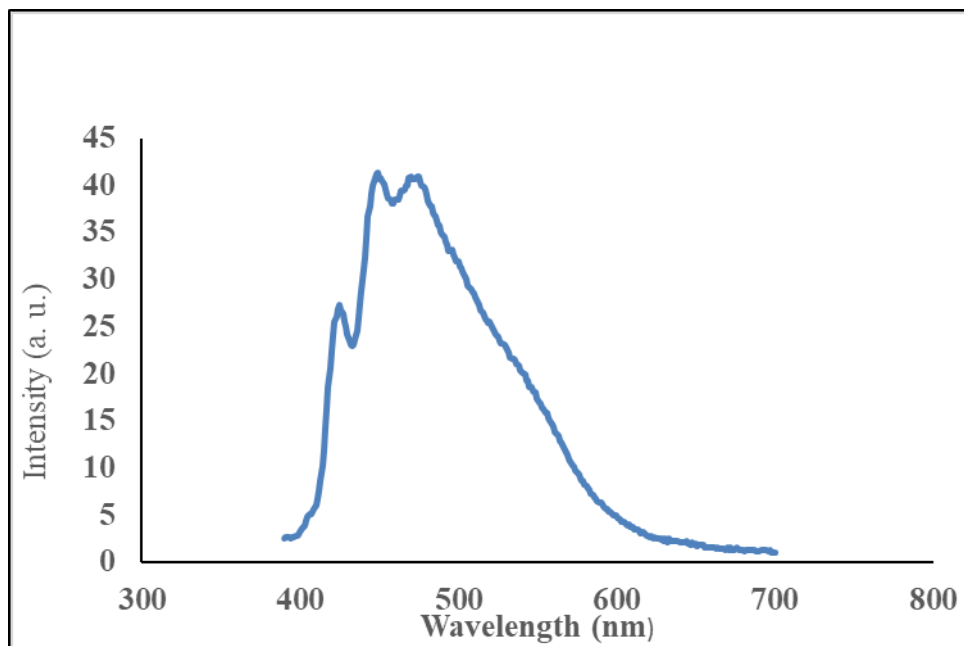


Figure 7: PL Spectra (Emission) for 8-HQ5-SAAF-II-C Copolymer Composites

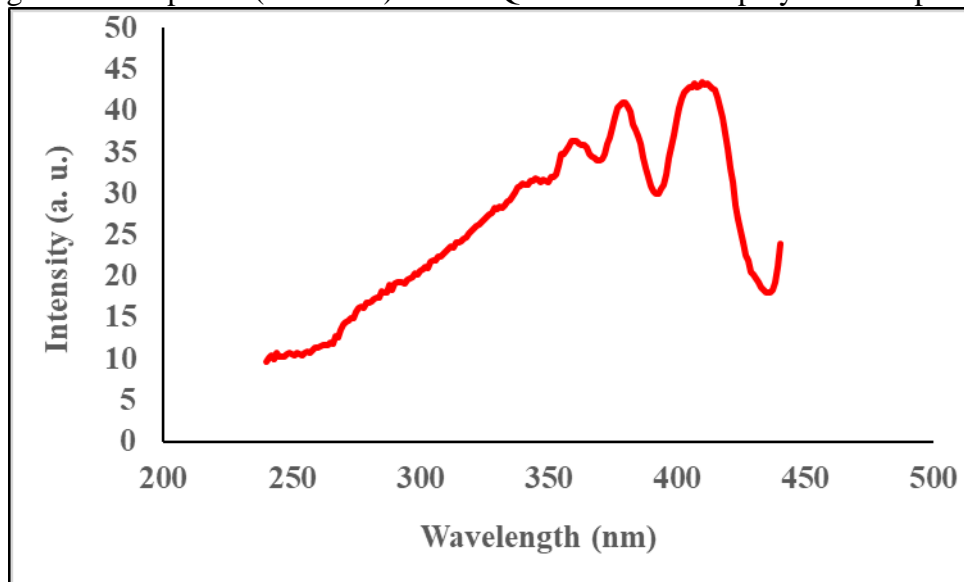


Figure 8: PL Spectra (Excitation) for 8-HQ5-SAAF-II-C Copolymer Composites

#### 4. Conclusion

In conclusion, we have effectively used polycondensation to create a novel functional copolymer. The spectral data change that was obtained suggested that the resultant polymers have a wide polymer. When compared to their copolymer, the composite TGA study results showed that they were more thermally stable. Copolymers have homogenous shape and randomly oriented crystallites, as seen in the SEM images. The copolymer photoluminescence spectra in solid powder were found to exhibit greenness at a maximum wavelength of 482 nm. As a result, the conducting copolymer-charcoal composites' PL

spectra demonstrate that the material was of sufficient quality to be used in semiconductor device research and serve as a support material for applications such as solid-state lighting and photoluminescent liquid crystal displays (PLLCDs).

#### References

1. Xu CJ, Li BG, Wan JT, Bu ZY. Design, synthesis and characterization of a highly luminescent Eu-complex monomer featuring thenoyltrifluoroacetone and 5-acryloxyethoxymethyl-8-hydroxyquinoline. Journal of

- luminescence. 2011 Aug 1;131(8):1566-70.
- Zhang H, Song H, Dong B, Han L, Pan G, Bai X, Fan L, Lu S, Zhao H, Wang F. Electrospinning preparation and luminescence properties of europium complex/polymer composite fibers. *The Journal of Physical Chemistry C*. 2008 Jun 26;112(25):9155-62.
  - Fang X, Zhai T, Gautam UK, Li L, Wu L, Bando Y, Golberg D. ZnS nanostructures: from synthesis to applications. *Progress in Materials Science*. 2011 Feb 1;56(2):175-287.
  - Wróblewska-Krepsztul J, Rydzkowski T, Borowski G, Szczypiński M, Klepka T, Thakur VK. Recent progress in biodegradable polymers and nanocomposite-based packaging materials for sustainable environment. *International Journal of Polymer Analysis and Characterization*. 2018 May 19;23(4):383-95.
  - Anwer AH, Ahtesham A, Shoeb M, Mashkoo F, Ansari MZ, Zhu S, Jeong C. State-of-the-art advances in nanocomposite and bio-nanocomposite polymeric materials: A comprehensive review. *Advances in colloid and interface science*. 2023 Jun 25:102955.
  - Yang Y, Yu M, Yan TT, Zhao ZH, Sha YL, Li ZJ. Characterization of multivalent lactose quantum dots and its application in carbohydrate-protein interactions study and cell imaging. *Bioorganic & medicinal chemistry*. 2010 Jul 15;18(14):5234-40.
  - Medintz IL, Uyeda HT, Goldman ER, Mattoussi H. Quantum dot bioconjugates for imaging, labelling and sensing. *Nature materials*. 2005 Jun 1;4(6):435-46.
  - Wang L, Sun Y, Xie X. Structural and optical properties of Cu nanoparticles formed in chitosan/sodium alginate multilayer films. *Luminescence*. 2014 May;29(3):288-92.
  - Wang L, Sun Y. Preparation and optical properties of alloyed ZnxCd1-xS nanoparticles. *Luminescence*. 2015 Feb;30(1):86-90.
  - Gupta PG, Gupta RH, Gurnule WB, Rao SN, Rathod YU. Synthesis, Characterization, and Photoluminescence Properties of 2-amino 6-nitrobenzothiazole-Melamine-Formaldehyde Copolymer-Charcoal Composite. *Indian Journal of Engineering & Materials Sciences* 2023 Dec;30(6):838-44.
  - Rathod YU, Pandit VU, Bhagat DS, Gurnule WB. Synthesis of copolymer and its composites with carbon and their photoluminescence studies. *Materials Today: Proceedings*. 2022 Jan 1;53:123-9.
  - Desai NK, Dongale TD, Kolekar GB, Patil SR. Synthesis, characterization, electrical and luminescence performance of novel copolymer of anthracene/pyrrole. *Journal of Materials Science: Materials in Electronics*. 2017 Apr;28:5116-27.
  - Hou ZZ, Yang QH, Li Y. Facile Synthesis of Pyrene/Pyrrole Copolymer with Strong Green Fluorescence. *Advanced Materials Research*. 2012 Mar 28;482:835-8.
  - Kim SH, Singu BS, Yoo KR, *Journal of Industrial Engineering Chemistry*. 2015; 30:174.
  - Katsoulidis AP, Dyar SM, Carmieli R, Malliakas CD, Wasielewski MR, Kanatzidis MG. Copolymerization of terephthalaldehyde with pyrrole, indole and carbazole gives microporous POFs functionalized with unpaired electrons. *Journal of Materials Chemistry A*. 2013;1(35):10465-73.
  - Chakole SP, Nandekar KA, Gurnule WB. Photoluminescent studies of 2, 2'-dihydroxybiphenyl, ethylenediamine-formaldehyde copolymer. In *Journal of Physics: Conference Series* 2021 May 1 (Vol. 1913, No. 1, p. 012062). IOP Publishing.
  - Gurnule WB, Rathod YU. Synthesis, Characterization and Thermal Behaviour Studies of Terpolymer Resin Derived from 8-Hydroxyquinoline-5-Sulphonic Acid and Anthranilic Acid. *CurrApplPolym Sci*. 2020;4:1-8.
  - RiswanAhamed MA, Azarudeen RS, Jeyakumar D, Burkanudeen AR.



- Terpolymer chelates: synthesis, characterization, and biological applications. *International Journal of Polymeric Materials*. 2010 Dec 17;60(2):124-43.
19. Yeole MM, Shrivastav AS, Gurnule WB, Der PharmaChemica. 2015;7(5):124-29.
20. Velmurugan G, Ahamed KR, Azarudeen RS. A novel comparative study: synthesis, characterization and thermal degradation kinetics of a terpolymer and its composite for the removal of heavy metals. *Iranian Polymer Journal*. 2015 Mar;24:229-42.
21. Gurnule WB, Rathod YU, Belsare AD, Das NC. Thermal degradation and antibacterial study of transition metal complexes derived from novel terpolymer ligand. *Materials Today: Proceedings*. 2020 Jan 1;29:1044-9.
22. Rathod YU, Zanje SB, Gurnule WB. Hydroxyquinoline copolymers synthesis, characterization and thermal degradation studies. In *Journal of Physics: Conference Series* 2021 May 1 (Vol. 1913, No. 1, p. 012061). IOP Publishing.
23. Azarudeen RS, Mohamed A, Ahamed MAR, Burkanudeen AR, Desalination. 2011;268:90-96.
24. Velmurugan G, Ahamed KR, Azarudeen RS, Thirumarimurugan M. Separations of toxic metal ions using a novel polymeric composite: Synthesis, characterizations, kinetics, isotherm models and thermal degradation studies. *Separation Science and Technology*. 2017 Aug 13;52(12):1946-58.
25. Gurnule WB, Vajpai KS, Mankar RV, Kohad CG. Photoluminescence studies of copolymer metal complexes with 8-hydroxyquinoline, hexamethylenediamine and formaldehyde. *Materials Today: Proceedings*. 2020 Jan 1;29:974-80.
26. Kohad CG, Gurnule WB, *Materials Today: Proceedings*. 2019 May;15(3):438-46.
27. Mandavgade SK, Gurnule WB. Synthesis and chelate ion exchange properties of copolymer resin: 8-hydroxyquinoline-5-sulphonic acid-catechol-formaldehyde. *Materials Today: Proceedings*. 2022 Jan 1;60:1814-8.
28. Chakole SP, Nandekar KA, Gurnule WB. Photoluminescent studies of 2, 2'-dihydroxybiphenyl, ethylenediamine-formaldehyde copolymer. In *Journal of Physics: Conference Series* 2021 May 1 (Vol. 1913, No. 1, p. 012062). IOP Publishing.
29. Gurnule WB, Vajpai KS, Mankar RV, Kohad CG. Photoluminescence studies of copolymer metal complexes with 8-hydroxyquinoline, hexamethylenediamine and formaldehyde. *Materials Today: Proceedings*. 2020 Jan 1;29:974-80.